Organic & Biomolecular Chemistry

Dynamic Article Links

Cite this: *Org. Biomol. Chem.*, 2012, **10**, 631

www.rsc.org/obc

PAPER

Solvent induced cooperativity of Zn(II) complexes cleaving a phosphate diester RNA analog in methanol†

Mark F. Mohamed, Irma Sánchez-Lombardo, Alexei A. Neverov and R. Stan Brown*

Received 29th August 2011, Accepted 14th October 2011
DOI: 10.1039/c1ob06482g

The kinetics of cyclization of 2-hydroxypropyl *p*-nitrophenyl phosphate (**1**) promoted by two mononuclear Zn(II) catalytic complexes of bis(2-pyridylmethyl)benzylamine (**4**) and bis(2-methyl 6-pyridylmethyl)benzylamine (**5**) in methanol were studied under $^{s}_{s}$pH-controlled conditions (where $^{s}_{s}$pH refers to [H^+] activity in methanol). Potentiometric titrations of the ligands in the absence and presence of Zn^{2+} and a non-reactive model for **1** (2-hydroxylpropyl isopropyl phosphate (HPIPP, **6**)) indicate that the phosphate is bound tightly to the **4**:Zn(II) and **5**:Zn(II) complexes as **L**:Zn(II):$\mathbf{6}^-$, and that each of these undergoes an additional ionization to produce **L**:Zn(II):$\mathbf{6}^-$:($^-OCH_3$) or a bound deprotonated form of the phosphate, **L**:Zn(II):$\mathbf{6}^{2-}$. Kinetic studies as a function of [**L**:Zn(II)] indicate that the rate is linear in [**L**:Zn(II)] at concentrations well above those required for complete binding of the substrate. Plots of the second order rate constants (defined as the gradient of the rate constant *vs.* [complex] plot) *vs.* $^{s}_{s}$pH in methanol are bell-shaped with rate maxima of 23 dm mol^{-1} s^{-1} and 146 dm mol^{-1} s^{-1} for **4**:Zn(II) and **5**:Zn(II), respectively, at their $^{s}_{s}$pH maxima of 10.5 and 10. A mechanism is proposed that involves binding of one molecule of complex to the phosphate to yield a poorly reactive 1 : 1 complex, which associates with a second molecule of complex to produce a transient cooperative 2 : 1 complex within which the cyclization of **1** is rapid. The observations support an effect of the reduced polarity solvent that encourages the cooperative association of phosphate and two independent mononuclear complexes to give a reactive entity.

Introduction

The enzymes responsible for the cleavage of the phosphate diester linkage (ROP(O_2^-)–OR′) in DNA and RNA are among the most efficient known, achieving accelerations for P–OR′ hydrolysis or transesterification of up to 10^{17} times.[1] Many such phosphodiesterase enzymes contain two or more metal ions in their active sites[2] which has spurred imaginative approaches to develop anthropogenic metallo-catalysts that are capable of ROP(O_2^-)–OR′ cleavage with enzyme-like efficiency.[3] Based on the notion that the effective dielectric constants of enzyme active sites resemble those of organic solvents rather than water,[4] we have initiated a program to investigate the ability of metal containing complexes to catalyze the reactions of phosphate diesters and triesters in the light alcohols.[5] These studies show that highly active dinuclear complexes can be generated in the light alcohols, methanol and ethanol, where they exhibit high levels of metal ion cooperativity for phosphate diester cleavage.[6] In an initial study,[7] we found that plots of the k_{obs} values for catalyzed intramolecular cyclization of the RNA model 2-hydroxypropyl-*p*-nitrophenyl phosphate (HPNPP, **1**) *vs.* [**2**:Zn(II):($^-OCH_3$)] in methanol exhibited upward curvature consistent with a process which is second order in [**2**:Zn(II)]. This suggested that a corresponding dinuclear complex such as **3**:$Zn(II)_2$ should have even greater activity, which proved to be the case, since the k_2^{obs} for its catalytic cleavage of **1** was 2.75×10^5 dm^3 mol^{-1} s^{-1}: this corresponds to an acceleration of ~10^8 over the methoxide-promoted reaction in methanol where $k_2^{MeO^-} = 2.56 \times 10^{-3}$ dm^3 mol^{-1} s^{-1}.[5a] It appears that the switch from water to a lower dielectric constant alcohol solvent provides at least three important effects that greatly accelerate M^{x+}:($^-$OR)-catalyzed phosphoryl transfer reactions. These are: (a) increasing the electrostatic ion–ion and ion–dipole association of the metal ion and oppositely charged or polarized substrates; (b) increasing the solubility of metal ions at 'pH' values above the 'pK_a' of the $M^{x+}(HOR)_n \rightleftharpoons M^{x+}(^-OR)(HOR)_m + H^+$ ionization; and, (c) providing a medium effect that accelerates the reactions where charge is dispersed in transition states.

The results in methanol are in stark contrast to the reported situation in water, the medium in which most of the work concerning synthetic metallo-nucleases has been conducted.[8] We have reviewed the problems associated with the study of metallo-complexes in water.[9] Under largely aqueous conditions, dinuclear complexes, including **3**:$Zn(II)_2$,[10] characteristically do not show any clear sign of metal ion cooperativity toward the cleavage

Department of Chemistry, Queen's University Kingston, Ontario, Canada, K7L 3N6. E-mail: rsbrown@chem.queensu.ca; Fax: +1-613-533-6669; Tel: +1-613-533-2400

† Electronic supplementary information (ESI) available: Tables and Figures giving various k_{obs} *vs.* [catalyst] rate constant data for cleavage of **1** as well as the ^{1}H NMR spectrum of **4**. See DOI: 10.1039/c1ob06482g

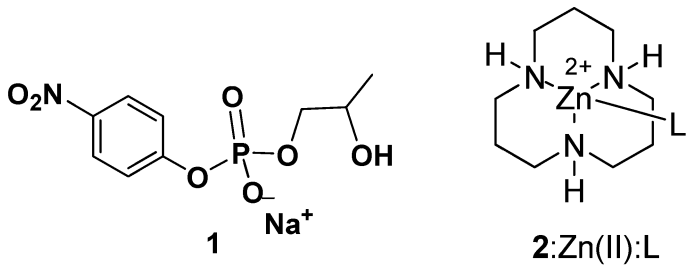

1

2:Zn(II):L

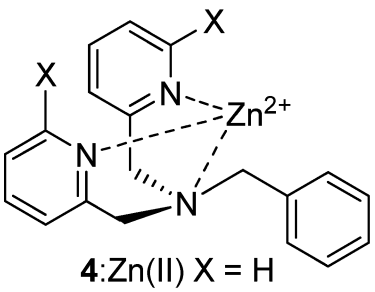

4:Zn(II) X = H

5:Zn(II) X = CH_3

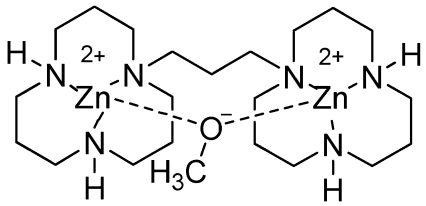

3:$Zn(II)_2$

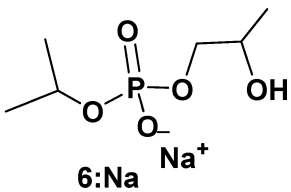

6:Na

of phosphate esters, and in many cases are not better than the hydroxide-promoted reaction in terms of second order rate constant. Albeit rare, there are standout cases[8c,g,11] where dinuclear complexes are over two orders of magnitude more reactive toward the cyclization of **1**, or cleavage of other phosphate diesters in water, than are the appropriate mononuclear comparison and the $^{-}$OH-promoted reaction.

To our knowledge, there are no reports of studies describing the aqueous reactivity of mononuclear complexes that promote the cleavage of phosphate esters where the kinetics are greater than first order in [complex].[12] The plot of k_{obs} *vs.* [**2**:Zn(II):L:$^{-}$OH] for the catalyzed cleavage of HPNPP in water is strictly linear, signifying no appreciable substrate binding nor kinetic terms higher than first order in catalyst.[12e] However, Deal and Burstyn[13] observed saturation kinetics for the hydrolysis of *O*-ethyl *O*-4-nitrophenyl phosphate promoted by the Cu(II) complex of 1,4,7-triazacyclononane, indicative of the formation of a kinetically active 1 : 1 catalyst:substrate complex with relatively weak binding (K_M = 0.062 mol dm^{-3}) with no evidence for a higher than first order dependence on [catalyst].

Although we have provided several examples of dinuclear complexes exhibiting strong metal ion cooperativity in methanol,[6,14,15] it is an open question whether the low polarity of alcohol solvents might prove more general in recruitment of two mononuclear complexes such as **2**:Zn(II) for cooperative cleavage of phosphate diesters.[6a,c] Herein, we report a kinetic and potentiometric titration study of the cyclization of **1** promoted by two other complexes in methanol, **4**:Zn(II) and **5**:Zn(II), where each system demonstrates such cooperativity. The present cases also demonstrate: (1) strong 1 : 1 binding between a mononuclear complex and substrate **1**; and, (2) that the medium facilitates a cooperative mechanism involving a transient 2 : 1 complex:substrate super-complex that promotes the intramolecular cyclization reaction of **1** at rates approaching what is achievable by dinuclear complexes where the catalytic units are covalently linked.

Experimental

(a) Materials

Methanol (DriSolv) was purchased from EMD Chemicals. $Zn(OTf)_2$ (98%), sodium methoxide (0.50 M solution in methanol, titrated against N/50 certified standard aqueous HCl solution and found to be 0.49 M), 2,6-lutidine (98%), *N*-methylpiperidine (99%), 4-ethylmorpholine (98%), triethylamine (99%), 2,2,6,6-tetramethylpiperidine (99%), trifluoromethanesulfonic acid, benzylamine (99%), and 2-picolylchloride hydrochloride (98%) were purchased from Aldrich and used without further purification. 2-Hydroxypropyl *iso*-propyl phosphate **6** was available from a previous study.[16]

(b) Synthesis

Bis(2-pyridylmethyl)benzylamine (4). Benzylamine (0.66 g, 0.006 mol) and 2-picolylchloride hydrochloride (2.07 g, 0.012 mol) were dissolved in 15 mL of water and heated to 60 °C in an oil bath. To the stirring mixture was added 7 mL of 5 N aqueous NaOH drop-wise, after which the mixture was stirred at 60 °C for one hour. The mixture was cooled to room temperature and then extracted with 3 × 20 mL CH_2Cl_2. The combined extracts were dried (Na_2SO_4) and then evaporated to give a brown oil. The crude product was purified by flash silica gel chromatography on a Biotage SP1 purification system, using $CHCl_3$/$HOCH_3$ (10 : 1) as the eluent (R_f 0.15). The purified product (1.3 g, 73% yield) was obtained as a yellow oil whose spectral characteristics were consistent with those previously published.[17]

^{1}H NMR (400 MHz, $CDCl_3$): shown in the ESI;† δ 8.53 (2H, d, J = 4 Hz), δ 7.67 (2H, t, J = 8 Hz), δ 7.60 (2H, d, J = 8 Hz), δ 7.42 (2H, d, J = 4 Hz), δ 7.33 (2H, t, J = 4 Hz), δ 7.24 (1H, t, J = 8 Hz), δ 7.15 (2H, t, J = 4 Hz), δ 3.82 (4H, s), δ 3.70 (2H, s). ^{13}C NMR (150 MHz, $CDCl_3$): δ 58.6, 60.0, 121.9 122.7, 127.1, 128.3, 128.8,

136.4, 138.9, 148.9, 159.8. HRMS (EI-TOF) calcd for $C_{19}H_{19}N_3$ (M^+): 289.1579; found 289.1592. $\lambda_{max}(HOCH_3)$ = 260 nm.

Bis(2-methyl 6-pyridylmethyl)benzylamine (5). To a suspension of 2-bromomethyl-6-methylpyridine[18] (2.29 g, 0.012 mol) in 15 mL of water was added benzylamine (0.64 mL, 0.0059 mol) and the mixture was heated with stirring to 60 °C. To this was added 10 mL of 5 N aqueous NaOH drop-wise, after which the mixture was stirred at 60 °C for one hour during which the mixture became clear. This was cooled to room temperature and then extracted with 2 × 20 mL CH_2Cl_2. The combined extracts were dried (Na_2SO_4) and then evaporated to give a viscous orange oil. The crude product was purified by flash silica gel chromatography on a Biotage SP1 purification system, using $CHCl_3/HOCH_3$ (40 : 1) as the eluent (R_f 0.15). The purified product (1.2 g, 65% yield) was obtained as a pale yellow oil which formed an off-white solid upon standing. Mp = 76–77 °C (lit. 76.9 °C[19]). ^{1}H NMR (300 MHz, $CDCl_3$): δ 7.57 (2H, t, J = 9 Hz), δ 7.45 (4H, dd, J = 9 Hz), δ 7.30 (3H, m), δ 7.00 (2H, d, J = 9 Hz), δ 3.80 (4H, s), δ 3.70 (2H, s), δ 2.53 (6H, s). ^{13}C NMR (150 MHz, $CDCl_3$): δ 24.8, 58.9, 60.5, 119.7, 121.7, 127.3, 128.6, 129.2, 137.0, 139.6, 157.8, 159.8. HRMS (EI-TOF) calcd for $C_{21}H_{23}N_3$ (M^+): 317.1892; found 317.1878. Anal. Calcd for $C_{21}H_{23}N_3$: C, 79.46; H, 7.30; N, 13.24. Found: C, 79.65; H, 7.20; N, 13.23. $\lambda_{max}(HOCH_3)$ = 270 nm.

(c) Kinetics

Kinetics in methanol using UV-Visible spectroscopy. The kinetics of catalyzed cleavage of **1** (5.0 × 10^{-5} mol dm^{-3} in methanol) were monitored by UV-vis spectrophotometry at 25.0 ± 0.1 °C by observing the rate of appearance of *p*-nitrophenol at 320 nm or *p*-nitrophenolate at 400 nm. First order rate constants (k_{obs}) were obtained from fitting the absorbance *vs.* time traces to a standard exponential model. All kinetic experiments were performed in quartz cuvettes with catalyst formed *in situ* through sequential addition of stock solutions (typically 1.0 × 10^{-1} mol dm^{-3}) of each of ligand and $Zn(OTf)_2$ to buffered methanol solutions to make a total volume of 2.5 mL. Reactions were initiated by the addition of substrate to this solution. Buffer solutions were prepared at 20.0 mmol dm^{-3} using the following amines and triflic acid (HOTf) in methanol to adjust the ^s_spH[20] of the solution (2,6-lutidine, ^s_spH = 7.60; *N*-ethylmorpholine, ^s_spH = 8.00–9.10; *N*-methylpiperidine, ^s_spH = 9.90; triethylamine, ^s_spH = 10.10–11.3; 2,2,6,6-tetramethylpiperidine, ^s_spH = 12.00–12.10). Where buffer inhibition was observed, plots of k_{obs} *vs.* $[buffer]_{total}$ were linear with a downward slope. Extrapolation of the plot of k_{obs} *vs.* $[buffer]_{total}$ to zero concentration gave a buffer-independent rate constant that was used to correct the original experimental data (see the ESI†). The reported values of the k_{obs} constants for the production of *p*-nitrophenol (phenolate) are the averages of duplicate runs.

The $[CH_3OH_2^+]$ was determined potentiometrically using a combination glass electrode (Radiometer model no. XC100-111-120-161) calibrated with certified standard aqueous buffers (pH = 4.00 and 10.00). The measured ^s_wpH meter readings in methanol were converted to the ^s_spH values by subtracting the δ correction factor of –2.24.[20]

(d) Potentiometric titrations

Titrations were performed in duplicate using an autotitrator equipped with an Accumet model 13-620-183 combination glass electrode calibrated with Fischer certified standard aqueous buffers (pH 4.00 and 10.00) as described.[6,14,15] Potentiometric titrations of **4**, **5**, $Zn(OTf)_2$ and the sodium salt of 2-hydroxylpropyl *iso*-propyl phosphate (HPIPP, **6**:**Na**) were performed under Ar in methanol at 25 °C. For the metal ion/ligand and metal ion/ligand/phosphate titration experiments the concentration of metal ion, ligand and phosphate were all 1 × 10^{-3} mol dm^{-3}, and the final concentration of added acid, HOTf, was 4 × 10^{-3} mol dm^{-3}. The total sample volume in all cases was 20.0 mL. Sodium methoxide titrant was calibrated by titrating Fischer certified standard HCl in water, with the endpoint taken to be ^w_wpH 7.

The potentiometric data were analyzed using the computer program Hyperquad 2000 (version 2.1 NT),[21] with the autoprotolysis constant of pure methanol taken to be $10^{-16.77}$ (mol dm^{-3})[2] at 25 °C. The dissociation constants for the species **4**-H^+_n or **5**-H^+_n (n = 1–3) were determined from the analysis of the potentiometric titration data at 1 × 10^{-3} mol dm^{-3} **4** or **5**. Titrations were performed in duplicate and were analyzed separately. The respective species formation constants were averaged and the resulting values were used as constants in the subsequent Hyperquad analysis of 1 : 1 **4**:Zn(II) or **5**:Zn(II) titrations. Similarly, formation constants for **L**:Zn(II), **L**($^-OCH_3$):Zn(II) and Zn(II):($^-OCH_3$)$_2$ (L = **4**,**5**) were determined from the analysis of the potentiometric titrations of 1 × 10^{-3} mol dm^{-3} $Zn(OTf)_2$ with an equimolar amount of **4** or **5**, and the resulting values were used as constants in the subsequent Hyperquad analysis of 1 : 1 : 1 **L**:Zn(II):Phos titrations.

Results

(i) Potentiometric titration and speciation analysis

Given in Table 1 are the various constants determined from the potentiometric titration of the L = **4** and **5** systems which were obtained as follows. For simplicity throughout, the various forms are depicted as **L**:Zn(II) when the Zn^{2+} is simply bound to the ligand, and **L**:Zn($^-OCH_3$), or **L**:Zn:Phos when the Zn^{2+} is bound to methoxide or to the anionic form of phosphate esters **6**$^-$ or **1**$^-$. Independent titrations of 1.0 mol dm^{-3} solutions of each

Table 1 Formation constants and acid dissociation constants for various species determined by potentiometric titration

Equilibrium	Log $^s_sK^a$ **L** = **4** system	Log $^s_sK^a$ **L** = **5** system
[**L**-H^+]↔[**L**][H^+]	–7.15 ± 0.02	–7.72 ± 0.02
[**L**][Zn]↔ [**L**:Zn]	7.0 ± 0.1	4.30 ± 0.05
[**L**][$^-OCH_3$][Zn]↔[**L**:Zn($^-OCH_3$)][^{b}]	14.01 ± 0.02	10.97 ± 0.03
[**L**:Zn($HOCH_3$)]↔[**L**:Zn($^-OCH_3$)][H^+][^{c}]	–9.76 ± 0.1	–10.10 ± 0.06
[**6**-H]↔[**6**$^-$][H^+]	–4.4 ± 0.3	–4.4 ± 0.3
[**L**][Zn][**6**$^-$]↔[**L**:Zn:**6**$^-$]	11.5 ± 0.3	9.00 ± 0.02
[**L**][Zn][$^-OCH_3$][**6**$^-$]↔[**L**:Zn($^-OCH_3$):**6**$^-$][^{d}]	18.07 ± 0.1	14.77 ± 0.01

[a] Derived from fits of the potentiometric titration data using the program Hyperquad 2000. Log ^s_sK refers to the log of the acid dissociation constant or the log of the equilibrium constant computed in the direction shown in column 1. [b] Defined as **L** + $^-OCH_3$ + Zn ⇌ **L**:Zn($^-OCH_3$), calculated from –16.77 + β values where –16.77 comes from the autoprotolysis constant of methanol of $10^{-16.77}$. [c] Computed from –16.77 + (log([**L**:Zn($^-OCH_3$)]/[**L**][$^-OCH_3$][Zn]) – log([**L**:Zn]/[**L**][Zn]). [d] Defined as **L** + $^-OCH_3$ + Zn + **6**$^-$ ⇌ **L**:Zn($^-OCH_3$):**6**$^-$, calculated from –16.77 + β values where –16.77 comes from the autoprotolysis constant of methanol of $10^{-16.77}$.

ligand were performed, providing the $^{s}_{s}pK_a$ values for the last acid dissociation step, of 7.15 ± 0.02 and 7.72 ± 0.02 for **4**-H$^+$ and **5**-H$^+$, respectively.

Analysis of the potentiometric titration profile data, as well as those for an equimolar mixture of $Zn(OTf)_2$ and **4** shown in Fig. 1, allow us to define the relevant species in solution as **4**:Zn(II) and **4**:Zn($^-OCH_3$), which, when fit *via* the Hyperquad 2000 program, provide log β values of 7.00 ± 0.06, and −2.76 ± 0.02. The formation constants for these two species were fixed for all subsequent analyses of the titration in the presence of HPIPP (**6**), a non-reactive structural model of HPNPP (**1**), and also for the fitting of the full titration profile for the former one, which produces a reasonable fit and provides respective stability constants for **4**:Zn:Phos and **4**:Zn:($^-OCH_3$):Phos species with log β values of 11.5 ± 0.3 and 1.3 ± 0.1. In Fig. 2 are titration profiles for **5** alone, as well as those for an equimolar solution of $Zn(OTf)_2$ with **5** and finally that of **5** with $Zn(OTf)_2$ in the presence of HPIPP. Hyperquad analysis of the data of the profile of **5** with $Zn(OTF)_2$ and the one for **5** alone, gives log β values of 4.3 ± 0.05 and −5.8 ± 0.03 for the species **5**:Zn(II) and **5**:Zn ($^-OCH_3$).

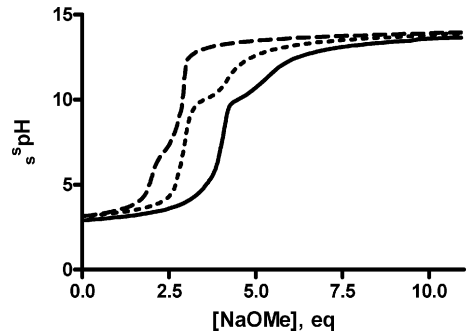

Fig. 1 Potentiometric titration profiles for 1 × 10^{-3} mol dm^{-3} **4** and 4 × 10^{-3} mol dm^{-3} HOTf, (---); the same in the presence of 1 × 10^{-3} mol dm^{-3} $Zn(OTf)_2$, (···); and 1 × 10^{-3} mol dm^{-3} **4** containing 4 × 10^{-3} mol dm^{-3} HOTf, 1 × 10^{-3} mol dm^{-3} of $Zn(OTf)_2$ and 1 × 10^{-3} mol dm^{-3} of HPIPP (—) in CH_3OH at 25 °C.

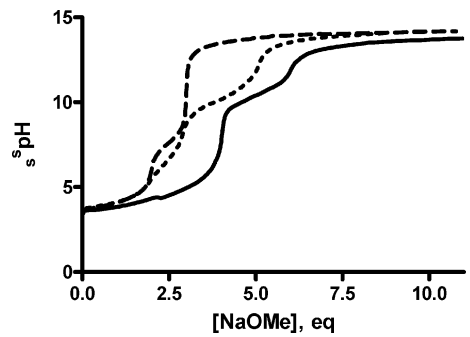

Fig. 2 Potentiometric titration profiles of 1 × 10^{-3} mol dm^{-3} **5** and 4 × 10^{-3} mol dm^{-3} HOTf, (---); the same in the presence of 1 × 10^{-3} mol dm^{-3} $Zn(OTf)_2$, (···); and 1 × 10^{-3} mol dm^{-3} **5** along with 4 × 10^{-3} mol dm^{-3} HOTf, 1 × 10^{-3} mol dm^{-3} of $Zn(OTf)_2$ and 1 × 10^{-3} mol dm^{-3} of HPIPP (—) in CH_3OH at 25 °C.

The speciation diagrams for the various forms of the **L**:Zn complex, Zn(II), and ligand were constructed using the constants given in Table 1, and are shown in Fig. 3 and 4. Fig. 3 indicates that, over the $^{s}_{s}$pH region used for the kinetics studies, more than

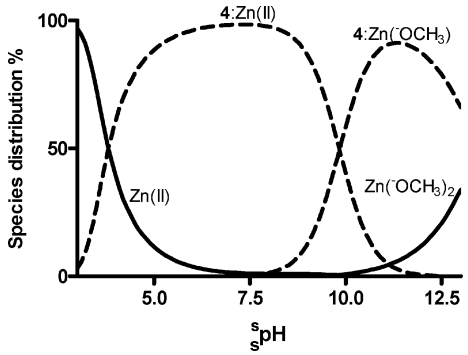

Fig. 3 Speciation diagram of various Zn(II) forms as a function of $^{s}_{s}$pH computed from the formation constants (given in the results section) under kinetic conditions of an equimolar solution of 1 × 10^{-3} mol dm^{-3} of $Zn(OTf)_2$ and **4** in methanol at 25 °C.

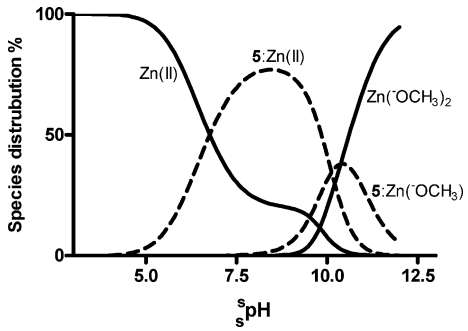

Fig. 4 Speciation diagram of various Zn(II) forms as a function of $^{s}_{s}$pH computed from the formation constants (given in the results section) under kinetic conditions of an equimolar solution of 1 × 10^{-3} mol dm^{-3} of $Zn(OTf)_2$ and **5** in methanol at 25 °C.

95% of the total Zn^{2+} is present as **4**:Zn(II) and **4**:Zn($^-OCH_3$) with the latter having a $^{s}_{s}pK_a$ of 9.76 for its formation. On the other hand, Fig. 4 shows that, with ligand **5**, the metal ion is not bound as tightly, with ~75% existing as **5**:Zn(II) at $^{s}_{s}$pH 8.5, and a maximum of 38% existing as **5**:Zn:($^-OCH_3$) at $^{s}_{s}$pH 10.4 ($^{s}_{s}pK_a$ for its formation 10.1). Above the latter $^{s}_{s}$pH, free Zn(II) in solution and that in **5**:Zn($^-OCH_3$) are sequestered further by methoxide to form $Zn(^-OCH_3)_2$.

Analysis of the data obtained for the titrations performed in the presence of HPIPP (**6**) provides respective stability constants for **L**:Zn:**6**$^-$ and **L**:Zn:($^-OCH_3$):**6**$^-$ or its chemical equivalent where the 2-hydroxypropyl group is deprotonated (**L**:Zn:**6**$^{2-}$). For the two ligand systems, the respective log β values for formation of the **L**:Zn:**6**$^-$ and **L**:Zn:($^-OCH_3$):**6**$^-$ forms are 11.5 and 1.3 for ligand **4** and 9.0 and −2.0 for ligand **5**. HPIPP (**6**) is used as a non-reactive model for the reactive substrate used in the kinetics (HPNPP (**1**)) to provide an approximate speciation diagram for the **L**:Zn:**1**$^-$ species with the understanding that the different structure and less electron withdrawing leaving group could alter the $^{s}_{s}$pH dependence of the various forms. The speciation diagrams for all the phosphate containing species shown in Fig. 5 and 6 were constructed using conditions relevant to the kinetics where [**4**] or [**5**] = [Zn(II)] = 1 × 10^{-3} mol dm^{-3} and [HPIPP] = 5 × 10^{-5} mol dm^{-3}. The concentration of the various [HPIPP] species in the presence of Zn(II) and **4** or **5** were subsequently computed as a function of the $^{s}_{s}$pH, inputting the $^{s}_{s}pK_a$ of HPIPP (4.4 ± 0.3), using HySS

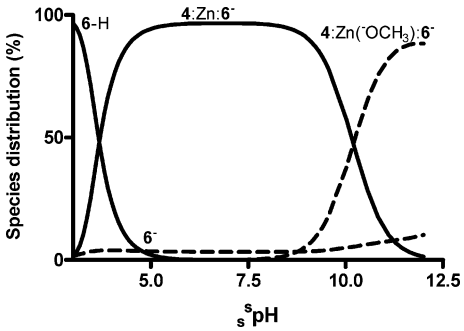

Fig. 5 Speciation diagram of various HPIPP forms as a function of ^{s}pH computed from the formation constants (given in the results section) under kinetic conditions of HPIPP 5×10^{-5} mol dm^{-3} in the presence of 1×10^{-3} mol dm^{-3} each of $Zn(OTf)_2$ and **4** in CH_3OH at 25 °C.

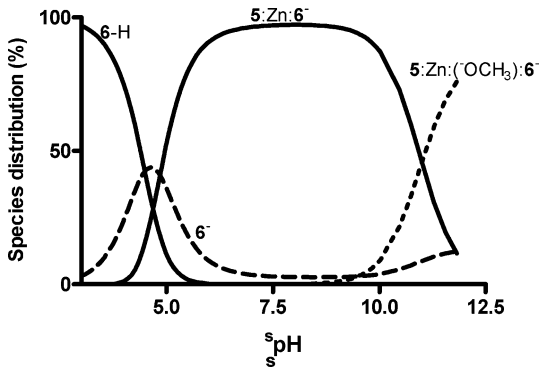

Fig. 6 Speciation diagram of various [HPIPP] forms as a function of ^{s}pH computed from the formation constants under kinetic conditions of HPIPP 5×10^{-5} mol dm^{-3} in the presence of 1×10^{-3} mol dm^{-3} each of $Zn(OTf)_2$ and **5** in CH_3OH at 25 °C.

2009. One sees, from the speciation diagram in Fig. 5 for ligand **4**, that between ^{s}pH 4.5 and 8, over 90% of the HPIPP phosphate diester is bound as **4**:Zn:**6**$^{-}$, and that above ^{s}pH 9.2 the bulk of the HPIPP exists predominantly **4**:Zn($^{-}$OCH$_3$):**6**$^{-}$ or its deprotonated phosphate form **4**:Zn:**6**$^{2-}$.

The speciation diagram in Fig. 4 for ligand **5** and Zn(II) shows that, in the absence of phosphate **6**, ~75% of the available Zn(II) is bound to the ligand as **5**:Zn(II) at ^{s}pH 7.8, and 50% is bound in that form at ^{s}pH 9.8, along with an additional 28% in the form of **5**:Zn:($^{-}$OCH$_3$). However, the speciation diagram in Fig. 6 for HPIPP along with **5** and Zn(II) as a function of ^{s}pH, shows that more than 90% of the HPIPP is fully bound as **5**:Zn:**6**$^{-}$ between ^{s}pH 5.9 and 9.8, and in the higher ^{s}pH region where the kinetic experiments were performed, over 90% of the HPIPP is present as **5**:Zn:**6**$^{-}$ and **5**:Zn:($^{-}$OCH$_3$):**6**$^{-}$ (or **5**:Zn:**6**$^{2-}$).

Fig. 7 and 8 present the observed first order kinetic data (k_{obs}) for the cleavage of HPNPP (**1**) *vs.* total [**4**:Zn(II)] or [**5**:Zn(II)], where the right *y*-axis gives the multiplication product of the calculated concentrations of [**4**:Zn:**6**$^{-}$][**4**:Zn:($^{-}$OCH$_3$)] at ^{s}pH 10.1 and [**5**:Zn:**6**$^{-}$][**5**:Zn:($^{-}$OCH$_3$)] at ^{s}pH 9.9, as determined from the potentiometric titration constants. The calculated concentrations of the species were computed using conditions where [HPIPP] = 5×10^{-5} mol dm^{-3} and [**4**:Zn(II)] or [**5**:Zn(II)] = 1×10^{-4}–2×10^{-3} mol dm^{-3}. Inspection of the plots in Fig. 7 and 8 shows that the k_{obs} values have excellent correlations with multiplication product

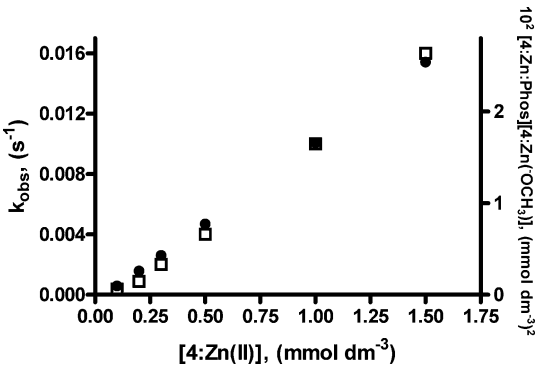

Fig. 7 Plot of k_{obs} *vs.* [**4**:Zn(II)] for the cleavage of HPNPP (**1**) (5×10^{-5} mol dm^{-3}) (□). Data superimposed on the figure as (●) are multiplication products of [**4**:Zn:**6**$^{-}$][**4**:Zn:($^{-}$OCH$_3$)] in accordance with the bimolecular reaction pathway given in Scheme 1, ^{s}pH 10.1 at 25 °C. The average value for the second order rate constant k_2^{cat} (Scheme 1) was calculated to be 24 ± 5 dm^3 mol^{-1} s^{-1}. For a discussion of this computed value and the observed second order rate constant for **4**, see below.

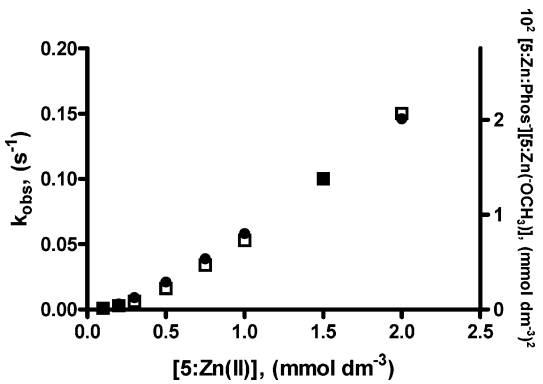

Fig. 8 Plot of k_{obs} *vs.* [**5**:Zn(II)] for the cleavage of HPNPP (**1**) (5×10^{-5} mol dm^{-3}) (□). Data superimposed on the figure as (●) are multiplication products of [**5**:Zn:**6**$^{-}$][**5**:Zn:($^{-}$OCH$_3$)] in accordance with the bimolecular reaction pathway given in Scheme 1, ^{s}pH 9.9 at 25 °C. The average value for the second order rate constant k_2^{cat} (Scheme 1) was calculated to be 316 ± 50 dm^3 mol^{-1} s^{-1}. For a discussion of this computed value and the observed second order rate constant for **5**, see below.

of [**L**:Zn:**6**$^{-}$][**L**:Zn:($^{-}$OCH$_3$)], which explains the upward curvature in the k_{obs} *vs.* [**L**:Zn(II)] kinetic plots shown later.

(ii) Dependence of the rate constant for cyclization of 1 on [L:Zn(II)] and ^{s}pH

The kinetics of the catalyzed cleavage of **1** were studied in buffered methanol with control of ^{s}pH and ionic strength. At all ^{s}pH values, plots of k_{obs} *vs.* [**4**:Zn(II)] or [**5**:Zn(II)] exhibited an upward curvature (see Fig. 7 and 8, and the ESI†). This is consistent with a process that is overall second order in [**L**:Zn(II)] or first order in each of [**L**:Zn(II)] and its ionization product, [**L**:Zn:($^{-}$OCH$_3$)]. Given in Scheme 1 is the favoured process where a tightly bound **L**:Zn:**1**$^{-}$ complex (predicted on the basis of the above potentiometric titration data) interacts productively with a second complex comprising **L**:Zn:($^{-}$OCH$_3$) to promote the catalytic cyclization of **1**. At high catalyst concentrations, higher than that which ensures formation of a 1 : 1 : 1 **L**:Zn:**1**$^{-}$ complex, the reactions are linear in [catalyst], suggesting the involvement

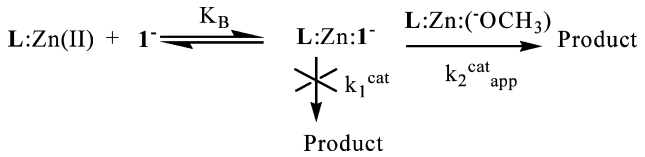

Scheme 1 L = **4**, **5**. Minimal scheme for the cyclization of **1** promoted by two equivalents of **L**:Zn(II).

Table 2 Computed apparent second order rate constants ($k_2^{cat}{}_{app}$) and dissociation constants (K_d) for the cyclization of HPNPP (**1**) catalyzed by **4**:Zn(II) at various ^s_spH values

^s_spH	$k_2^{cat}{}_{app}$ (dm^3 mol^{-1} s^{-1})	K_d (mmol dm^{-3})
8.0	0.180 ± 0.001	0.20 ± 0.06
8.5	0.850 ± 0.002	0.17 ± 0.04
9.1	2.87 ± 0.01	0.13 ± 0.03
10.1	17 ± 3	0.4 ± 0.16
10.8	15 ± 1	0.1 ± 0.02
11.3	10.6 ± 0.6	—
12.1	7.7 ± 0.1	—

Table 3 Computed apparent second order rate constants ($k_2^{cat}{}_{app}$) and dissociation constants (K_d) for the cyclization of HPNPP (**1**) catalyzed by **5**:Zn(II) at various ^s_spH values

^s_spH	$k_2^{cat}{}_{app}$ (dm^3 mol^{-1} s^{-1})	K_d (mmol dm^{-3})
7.6	10.8 ± 0.9	1.97 ± 0.20
8.3	32.9 ± 1.6	1.37 ± 0.15
8.6	43.6 ± 1.7	0.64 ± 0.09
8.9	79.2 ± 1.4	1.00 ± 0.05
9.9	137.0 ± 2.4	1.47 ± 0.06
10.4	105.2 ± 8.8	3.09 ± 0.41
10.9	43.9 ± 4.6	1.42 ± 0.34
11.2	30.0 ± 1.5	0.73 ± 0.12
12.0	5.6 ± 0.6	0.93 ± 0.26

of a second catalyst molecule in the mechanism for cleavage of **1**$^-$. The kinetic data were fit to eqn (1), derived for the process in Scheme 1, which incorporates a universal binding equation.[6,14,15] This gives the **L**:Zn:**1**$^-$ ⇌ **L**:Zn(II) + **1**$^-$ dissociation constant (K_d, taken as the reciprocal of the binding constant, K_B, from eqn (1)) as well as the apparent second order rate constant for the reaction between the **L**:Zn:**1**$^-$ complex and free catalyst ($k_2^{cat}{}_{app}$). Note that in the fit of the data it is not necessary to include the term k_1^{cat} for the unimolecular breakdown of the **L**:Zn:**1**$^-$ complex, suggesting that under the present conditions, this is too slow to be of any real kinetic benefit.

$$k_{obs} = k_2^{cat}{}_{app}([Cat] - (1 + K_B \times [S] + [Cat] \times K_B - X)/(2K_B)/[S]) \times (1 + K_B \times [S] + [Cat] \times K_B - X)/(2K_B)/[S]) \quad (1)$$

where:

$$X = (1 + 2K_B \times [S] + 2 \times [Cat] \times K_B + K_B{}^2 \times [S]^2 - 2 \times K_B{}^2 \times [Cat][S] + [Cat]^2 \times K_B{}^2)^{0.5}$$

The constants derived from the fittings for the rate constants for cyclization of **1** promoted by **4**:Zn(II) and **5**:Zn(II) as a function of ^s_spH are presented in Tables 2 and 3. The observed log $k_2^{cat}{}_{app}$ *vs.* ^s_spH plots for the two catalyst complexes are given in Fig. 9. Over the ^s_spH range studied, **4**:Zn(II) shows an increase in activity up to ^s_spH ~ 10.5 at which point k_2^{cat} decreases. The bell-shaped ^s_spH–rate data for both **4** and **5** were fit to eqn (2) (developed for a hypothetical process with three species interconnected by two

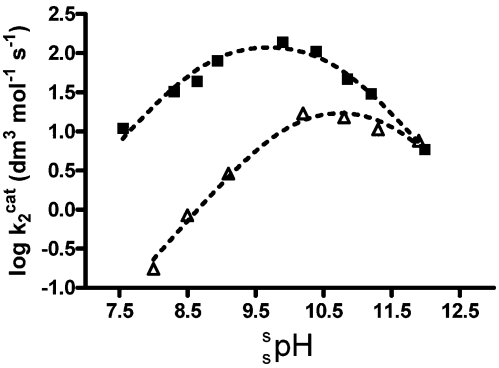

Fig. 9 Plots of log $k_2^{cat}{}_{app}$ *vs.* ^s_spH for the cyclization of **1** (5.0×10^{-5} mol dm^{-3}) catalyzed by **4**:Zn(II) (△) and **5**:Zn(II) (■) in buffered methanol at $T = 25.0 \pm 0.1$ °C. Lines through the data are obtained from fits to eqn (2).

ionizations where the active form of the catalyst is formed after the first ionization of the complex, and an inactive form formed after the second ionization). The fitting gives two apparent acid dissociation constants and a maximum apparent second order rate constant ($k_2^{cat}{}_{app}$)^{max} for **4**:Zn(II) of $^s_s pK_a^1 = 10.2 \pm 0.2$; $^s_s pK_a^2 = 11.5 \pm 0.15$; ($k_2^{cat}{}_{app}$)^{max} = 23.1 dm^3 mol^{-1} s^{-1} and for **5**:Zn(II), $^s_s pK_a^1 = 8.8 \pm 0.1$; $^s_s pK_a^2 = 10.6 \pm 0.1$; ($k_2^{cat}{}_{app}$)^{max} = 146.1 dm^3 mol^{-1} s^{-1}

$$k_2^{cat}{}_{app} = \left(\frac{(k_2^{cat}{}_{app})^{max}\, {}^s_s K_a^1 [H^+]}{[H^+]^2 + [H^+]\, {}^s_s K_a^1 + {}^s_s K_a^1\, {}^s_s K_a^2} \right) \quad (2)$$

The superpositionings of the data for log $k_2^{cat}{}_{app}$ *vs.* ^s_spH for the cyclization of **1** (5.0×10^{-5} mol dm^{-3}) catalyzed by **4**:Zn(II) and **5**:Zn(II) in buffered methanol at T = 25.0 ± 0.1 °C are shown in Fig. 39S and 40S of the ESI,† and are seen to correlate well with the computed concentration profiles as a function of ^s_spH for the multiplication product of [**L**:Zn(II):**6**][**L**:Zn(⁻OCH$_3$)]. Bearing in mind that the potentiometric and kinetic data are obtained under different conditions (buffered conditions with **1** for kinetics and non-buffered conditions with **6** for titrations), the Fig. 39S† concentration plot, constructed considering only the latter two species as the active forms, fits the ascending data at low ^s_spH well, but undershoots the $k_2^{cat}{}_{app}$ *vs.* ^s_spH data for **4** suggesting that some other species is active for catalysis at ^s_spH > 10. With **5**:Zn(II), the similar plot shown in Fig. 40S† fits the available kinetic acceptably well. Strong binding of an alternative anionic phosphate diester (dibenzyl phosphate) to these complexes is also demonstrated by an inhibition of the reaction of complex with a non-binding substrate (*O*-4-nitrophenyl *O*-ethyl methylphosphonate) shown in the ESI (Table 15S, Fig. 15S, and Table 35S, Fig. 35S).†

(iii) Turnover experiments for the cleavage of 1 catalyzed by 4:Zn(II) and 5:Zn(II)

Kinetic experiments were performed where the [**1**] = 10[**4**:Zn(II)] or 10[**5**:Zn(II)]. Since the potentiometric titration data with the poorly reactive, but similarly binding **6**, indicate that essentially all the phosphate is fully bound to **L**:Zn(II), in the absence of free catalyst the rate of reaction should be that of the unimolecular conversion of **L**:Zn:**1** to product (k_1^{cat}, Scheme 1). Reactions were performed in buffered methanol (as described above) with [**L**:Zn(II)] = 5.0×10^{-5} mol dm^{-3} and [**1**] = 5.0×10^{-4} mol dm^{-3}. The absorbance *vs.* time plots were fit to a standard first order exponential model

to obtain the k_1^{cat} rate constants, but for very slow reactions the rate constants were determined from initial rates by dividing the slope of the linear portion of the first 5–10% of the absorbance *vs.* time plots by the total expected absorbance change. The rate constants determined from the absorbance *vs.* time plots were multiplied by ten to account for the turnover number. The so-determined values of k_1^{cat} as a function of $_s^s$pH for **4**:Zn(II) and **5**:Zn(II) are summarized in the ESI (Table 16S and Table 36S, respectively†) along with plots of log k_1^{cat} *vs.* $_s^s$pH (Fig. 16S and Fig. 36S, respectively†).

Discussion

(a) Catalyst–substrate binding

The feature of note for the kinetics of cyclization of **1** catalyzed by **4**:Zn(II) and **5**:Zn(II) in methanol is the upward curvature in the k_{obs} *vs.* [catalyst] plots which signifies the involvement of two **L**:Zn(II) species cooperating to promoted the cleavage of **1**. Previous reports describing the kinetics of mononuclear Zn(II) complexes catalyzing the cleavage of phosphate diesters in water[12] do not indicate there are terms greater than first order in [catalyst] that would signify cooperation between two, non-tethered metal centers. Comparison of the speciation diagrams of Fig. 3 and 4 clearly shows that **4** binds the Zn(II) more fully than does **5**. This is consistent with steric effects exerted by the additional methyl groups in **5**:Zn(II) that encumber the Zn(II) centre. The binding constants of **1** to both **4**:Zn(II) and **5**:Zn(II), while subject to appreciable errors from fits of the kinetic data to eqn (1), are relatively insensitive to $_s^s$pH. The speciation diagrams in Fig. 5 and 6 indicate that **4**:Zn(II) and **5**:Zn(II) bind **6** (and presumably **1** as its anionic $ROPO_2^-$(OAr) form) nearly completely between $_s^s$pH 4–9 and 6–10, respectively. Nevertheless, from the $_s^s$pH/log $k_2^{cat}{}_{app}$ profiles shown in Fig. 9, the dominant reaction pathway (discussed in more detail below) apparently involves **L**:Zn:**1** reacting with a second molecule of catalyst in its basic form (**L**:Zn($^-$OCH$_3$)) up to $_s^s$pH 10–10.5, after which the catalysis drops due to the fact that free methoxide extracts Zn^{2+} from the various complexes forming Zn($^-$OCH$_3$)$_2$ or some oligomeric form thereof. With **4**, the two components of the **4**:Zn(II) ⇌ **4**:Zn($^-$OCH$_3$) + H$^+$ equilibrium ($_s^s$pK_a = 9.76) and **4**:Zn(II):**6** ⇌ **4**:Zn:($^-$OCH$_3$):**6** + H$^+$ equilibrium ($_s^s$pK_a ~10) account for ~95% of the Zn(II)-containing material up to $_s^s$pH 11 and 12, respectively, above which formation of Zn($^-$OCH$_3$)$_2$ becomes prominent. With **5**, which binds Zn(II) somewhat weaker than does **4**, the **5**:Zn(II) ⇌ **5**:Zn:($^-$OCH$_3$) + H$^+$ ⇌ Zn($^-$OCH$_3$)$_2$ equilibrium is such that nearly equal concentrations of these three components exist at $_s^s$pH 10.2, with [Zn($^-$OCH$_3$)$_2$] increasing sharply at higher values. Interestingly, the presence of phosphate tends to stabilize the **5**:Zn:**6** complexes so that the two components of the **5**:Zn(II):**6** ⇌ **5**:Zn:($^-$OCH$_3$):**6** + H$^+$ equilibrium ($_s^s$pK_a ~11) comprise about 85–90% of the phosphate-containing species up to $_s^s$pH 12. The complexity of speciation at high $_s^s$pH indicates that it is an oversimplification to describe the kinetic behaviors shown in Fig. 9 in terms of a process involving just three species interconnected by two $_s^s$pK_a values, particularly at high $_s^s$pH where Zn($^-$OCH$_3$)$_2$ becomes an important species. Nevertheless, this minimalistic approach serves to describe the kinetic behaviour on the low $_s^s$pH side up to the plateau region.

(b) Cyclization of 1 catalyzed by 4:Zn(II) and 5:Zn(II)

Aside from being strongly bound to the **L**:Zn(II) complexes, the cleavage of the anionic phosphate diester **1** catalyzed by **4**:Zn(II) and **5**:Zn(II) is distinguished by the cooperative behaviour of two catalyst complexes. The constants listed in Table 2 and Table 3 are apparent second order rate constants for the reaction between the **L**:Zn:**1** complex and a second complex comprising one or more of the non-phosphate bound forms of the catalyst, collectively represented as [**L**:Zn]$_{free}$ ($k_2^{cat}{}_{app}$ in Scheme 2), as derived from fitting the kinetic data to eqn (1). To determine if the reaction pathway involving only one molecule of catalyst (k_1^{cat} in Scheme 1) contributes significantly to the overall rate, we also performed turnover experiments using a large excess of substrate (see the ESI, Tables 16S, 36S and Fig. 16S, 36S). Under these conditions, the catalyst is expected to be fully bound to substrate and the observed first order rate constant refers to conversion of the **L**:Zn:**1** complex (with or without added methoxide) to product (k_1^{cat}). At the $_s^s$pH maximum of 9.9 for complex **5**:Zn(II), the observed rate constant (k_1^{cat}) determined at 0.05×10^{-3} mol dm^{-3} **5**:Zn(II) and 0.5×10^{-3} mol dm^{-3} **1** was 9.1×10^{-4} s^{-1}. Compared to the observed pseudo first order rate constant of k_{obs} = 0.15 s^{-1} for the cleavage of 5×10^{-5} mol dm^{-3} **1** catalyzed by excess **5**:Zn(II) (2.0×10^{-3} mol dm^{-3}) at $_s^s$pH = 9.9, the pathway with a single catalyst molecule is found to account for only 0.6% of the overall rate under these conditions A similar analysis for **4**:Zn(II) operating at its optimal $_s^s$pH of 12.0 shows that at [**4**:Zn(II)] = 1.5×10^{-3} mol dm^{-3}, only 4.7% of the reaction rate is due to the k_1^{cat} pathway. For our purposes, the unimolecular decomposition of **L**:Zn:**1** can therefore be ignored as a significant contributor to the reaction rate.

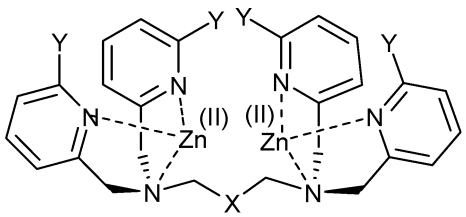

7:Zn(II)$_2$ X = (1,3-C$_6$H$_4$), Y = H
8:Zn(II)$_2$ X = (1,3-C$_6$H$_4$), Y = CH$_3$
9:Zn(II)$_2$ X = CH$_2$, Y = H
10:Zn(II)$_2$ X = CH$_2$, Y = CH$_3$

The cyclization of **1**, bound as a **L**:Zn:**1** complex that reacts with a second **4**:Zn(II) or **5**:Zn(II), is significantly accelerated relative to the methoxide-promoted background reaction of **1**. The maximal second order rate constants exhibited by **4**:Zn(II) and **5**:Zn(II), as determined from the fits in Fig. 9 (23.1 ± 2.5 dm^3 mol^{-1} s^{-1} and 146.1 ± 30.0 dm^3 mol^{-1} s^{-1}, respectively), are over 10^4 greater than the second order rate constant for the methoxide-promoted cleavage of **1** ($k_2^{OMe} = 2.56 \times 10^{-3}$ dm^3 mol^{-1} s^{-1}).[22] The addition of the methyl substituents in **5**:Zn(II) provides at most a factor of five rate enhancement compared to **4**:Zn(II). This can be compared with the results of a similar study of the cleavage of **1** promoted by dinuclear complexes[15] where the dinuclear complex **8**:Zn(II)$_2$ was over 10 times more reactive than complex **7**:Zn(II)$_2$ and complex **10**:Zn(II)$_2$ was over 10^3 more reactive than **9**:Zn(II)$_2$.

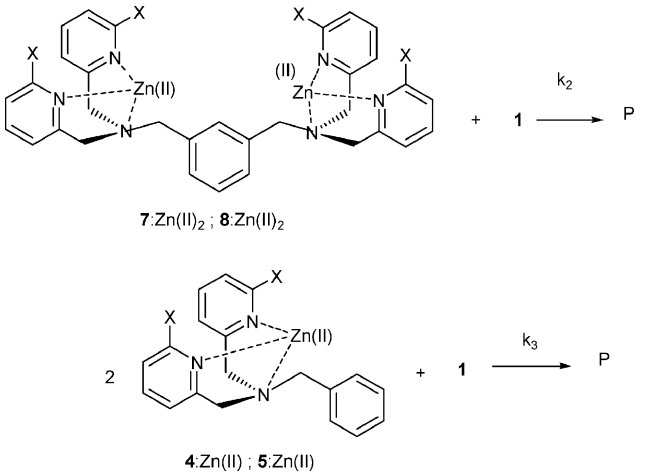

Scheme 2 Comparative systems for determining effective molarity (EM).

(c) Effective molarities of 4:Zn(II) and 5:Zn(II)

A comparison of the catalysis afforded by complexes **4**:Zn(II) and **5**:Zn(II) with that provided by the respective dinuclear counterparts (**7**:$Zn(II)_2$ and **8**:$Zn(II)_2$) quantifies the cooperative mechanism in terms of the effective molarity (EM). As generally applied, EM describes the efficiency of a system exhibiting an intramolecular unimolecular catalytic effect relative to a bimolecular process and is defined as the quotient of the first order rate constant for the intramolecular reaction divided by the second order rate constant for the intermolecular reaction proceeding by a comparable mechanism.[23] EM has units of concentration and represents the hypothetical [catalytic species] required for the intermolecular reaction to occur at the same rate as the intramolecular one. EM values as high as 10^{10} mol dm^{-3} [23c] are obtained for intramolecular nucleophilic catalysis, while for intramolecular general base catalysis the EM is generally much lower with limiting values of 100 mol dm^{-3}, but most examples being < 1.0 mol dm^{-3}.[24]

The EM values here are computed in a slightly different way, comparing the apparent second order rate constants for the reaction of the dinuclear catalysts (**7**:$Zn(II)_2$ and **8**:$Zn(II)_2$) with substrate **1** (k_2, Scheme 2) with the apparent third order rate constant for the reaction between **1** and two molecules of the mononuclear catalysts (**4**:Zn(II) and **5**:Zn(II)) (k_3 in Scheme 2). These EM values still represent the concentration of the mononuclear catalyst that would be necessary to achieve the same reaction rate as the analogous dinuclear complex. The third order rate constants for the reaction between **4**:Zn(II) and **5**:Zn(II) with **L**:Zn:**1** are defined as $k_3 = (k_2^{cat}{}_{app})^{max}/K_d$ where $(k_2^{cat}{}_{app})^{max}$ is the maximal second order rate constant for the reaction between the **L**:Zn:**1** complex and a second molecule of **L**:Zn(II) obtained by fitting the data in Tables 1 and 2 to eqn (2). K_d refers to the average catalyst:substrate dissociation constant (averaged from data in Tables 2 and 3). The respective third order rate constants (k_3) for **4**:Zn(II) and **5**:Zn(II) with **L**:Zn:**1** are $(23.1\ dm^3\ mol^{-1}s^{-1})/(1.0\times10^{-4}\ mol\ dm^{-3}) = 2.3\times10^5\ dm^6\ mol^{-2}\ s^{-1}$ and $(146.1\ dm^3\ mol^{-1}s^{-1})/(1.0\times10^{-3}\ mol\ dm^{-3}) = 1.5\times10^5\ dm^6\ mol^{-2}\ s^{-1}$, respectively, at the maxima of their respective ${}^s_spH$/rate profiles. The second order rate constants for the reaction of the dinuclear catalysts with **1** are defined as $k_2 = k_{cat}/K_M$, derived from the Michaelis–Menten plots observed for **7**:$Zn(II)_2$ and **8**:$Zn(II)_2$, and were previously determined to be $1.6\times10^3\ dm^3\ mol^{-1}\ s^{-1}$ and $29.8\times10^3\ dm^3\ mol^{-1}\ s^{-1}$, respectively.[15] The EM values based on this analysis are thus $EM_4 = 7\times10^{-3}$ mol dm^{-3} and $EM_5 = 2\times10^{-1}$ mol dm^{-3}.

The low values of EM obtained here for **4**:Zn(II) and **5**:Zn(II) can be interpreted in one of two ways: (1) a poor dinuclear catalyst (small k_2, Scheme 2); or (2) more likely, a very effective cooperativity in the mononuclear catalyst (large k_3, Scheme 2). To address the first possibility, under optimal ${}^s_spH$ conditions (${}^s_spH$ = 8.0), the saturating rate constant for the unimolecular decomposition of **8**:$Zn(II)_2$:**1** was previously[15] found to be $k_{cat}{}^{max} = 6.2\ s^{-1}$ while in the present study, the unimolecular decomposition of the **5**:Zn(II):**1** complex at the optimum ${}^s_spH$ of 10.8 is $k_1{}^{cat} = 0.0023\ s^{-1}$ (ESI, Table 36S). This comparison shows that when bound to substrate **1**, **5**:Zn(II) is nearly 2700-fold less active than the dinuclear species.

The low values of EM for **4**:Zn(II) and **5**:Zn(II) must therefore result from the high efficiency of the cooperative behaviour of the two mononuclear complexes. The binding of the first **L**:Zn(II) catalyst to the substrate, while not producing a very active form of **L**:Zn:**1**, activates the bound substrate in the latter toward further catalysis by **L**:Zn(II). This is particularly evident in the case of **4**:Zn(II) where the computed EM (7×10^{-3} mol dm^{-3}) lies well within a practically attainable concentration range. This suggests that, unlike the situation in water, where no catalyst cooperativity has ever been observed, the use of methanol as a solvent seems to predispose mononuclear Zn(II) complexes to cooperate in the cleavage of diester **1**, generating a catalytic system which approaches the efficiency of dinuclear systems where the two metal ions are physically connected.

Unfortunately, it is difficult to compare our EM values with those for other synthetic catalysts in water since no reports are available of mononuclear systems that exhibit such cooperativity. In comparison to our own previous work, the EM values for the catalytic systems reported here are much lower than the one that we now compute for complex **2**:Zn(II), the first mononuclear catalyst for which we observed evidence for catalyst cooperativity.[6a] Comparing the second order rate constant for the cleavage of **1** catalyzed by **3**:$Zn(II)_2$ ($2.75\times10^5\ dm^3\ mol^{-1}\ s^{-1}$) with the third order rate constant for the reaction of two equivalents of **2**:Zn(II) with substrate **1** ($1.8\times10^3\ dm^6\ mol^{-2}\ s^{-1}$), gives EM = 153 mol dm^{-3}. The very large EM for **2**:Zn(II) is a function of the very large catalysis afforded by the dinuclear catalyst and the much weaker cooperativity of the mononuclear complex. Unlike the situation with **4**:Zn(II) and **5**:Zn(II), the efficiency of the cooperativity with **2**:Zn(II) is limited by poor binding to substrate **1**, since saturation binding between this substrate and **2**:Zn(II) is not observed.

Conclusion

The present study in methanol, and previous ones from our labs concerning the metal ion promoted cleavage of phosphate diesters in alcohol, might be criticized for the apparent failing of the solvent model of an alcohol relative to the apparent situation in enzymes where the gross medium is water. This criticism can be challenged by pointing out that numerous biological processes involving acyl or phosphoryl transfer processes are really transesterifications, as exemplified by cleavages of RNA where a 2′-hydroxyl on a ribose is deprotonated to attack a 3′-phosphate cleaving it to a 2′,3′-cyclic phosphate. Secondly, the active site of the enzymes

promoting such reactions have reduced polarities, akin to those of the light alcohols, as well as being quite deficient in water content, thus being more like a molecular bottle, the insides of which are adorned with specific functional groups that are important to the catalytic process at hand. In the simplified biomimetic examples, the intramolecular cyclization of **1** serves as a highly simplified model for numerous studies in water and also for our studies in alcohol, where the major effects are greater binding constants promoted by the medium, and also very much lower transition state energies for the metal catalyzed phosphoryl transfer reaction. We previously rationalized the large rate accelerations observed for the cleavage of phosphate diesters catalyzed by dinuclear Zn(II) complexes in methanol[6,14,15] on the basis of several factors, the most important of which are: (1) enhanced association of the metal complex and substrate; (2) double activation of the substrate through Zn(II)$\cdots$O$^-$–P(OR)OAr–O$\cdots$Zn(II) binding; and (3) lowering the activation barrier for the transesterification by a synergistic medium effect that stabilizes a transition state of a transforming $Zn(II)_2$-bound substrate where there is more charge dispersal than in the ground state. The current study highlights additional, less appreciated but none-the-less beneficial aspects of alcohol solvent, namely promoting cooperative behaviour among mononuclear Zn(II) complexes. The observation of strong binding between a mononuclear Zn(II) complex and a phosphate diester is rare in water, but apparently far more common in a reduced dielectric alcohol medium such as methanol or ethanol.[25] We propose here an additional and perhaps far more common than realized aspect, namely the emergence of cooperative mechanisms involving initial strong binding between the metal complexes and anionic substrates like **1** followed by transient association of a second molecule of catalyst to induce the catalytic transformation of the substrate.

Acknowledgements

The authors gratefully acknowledge the generous support of the Natural Sciences and Engineering Research Council of Canada (NSERC). In addition M. F. M. acknowledges the receipt of an NSERC Alexander Graham Bell postgraduate scholarship (CGS-D). The authors are grateful to Mr Scott Strum who performed some preliminary experiments.

References

1 G. K. Schroeder, C. Lad, P. Wyman, N. H. Williams and R. Wolfenden, *Proc. Natl. Acad. Sci. U. S. A.*, 2006, **103**, 4052.
2 (*a*) W. N. Lipscomb and N. Sträter, *Chem. Rev.*, 1996, **96**, 2375; (*b*) J. A. Cowan, *Chem. Rev.*, 1998, **98**, 1067; (*c*) W. W. Cleland and A. C. Hengge, *Chem. Rev.*, 2006, **106**, 3252; (*d*) N. Sträter, W. N. Lipscomb, T. Klabunde and B. Krebs, *Angew. Chem., Int. Ed. Engl.*, 1996, **35**, 2024; (*e*) D. E. Wilcox, *Chem. Rev.*, 1996, **96**, 2435; (*f*) R. Krämer, *Coord. Chem. Rev.*, 1999, **182**, 243.
3 For some recent reviews see: (*a*) F. Mancin and P. Tecilla, *New J. Chem.*, 2007, **31**, 800; (*b*) J. R. Morrow, *Comments Inorg. Chem.*, 2008, **29**, 169; (*c*) M. Livieri, F. Mancin, G. Saielli, J. Chin and U. Tonellato, *Chem.–Eur. J.*, 2007, **13**, 2246.
4 (*a*) W. W. Cleland, P. A. Frey and J. A. Gerlt, *J. Biol. Chem.*, 1998, **273**, 25529; (*b*) T. Simonson, F. Carlsson and D. A. Case, *J. Am. Chem. Soc.*, 2004, **126**, 4167 and references therein; (*c*) J. P. Richard and T. L. Amyes, *Bioorg. Chem.*, 2004, **32**, 354.
5 (*a*) A. A. Neverov, Z.-L. Lu, C. I. Maxwell, M. F. Mohamed, C. J. White, J. S. W. Tsang and R. S. Brown, *J. Am. Chem. Soc.*, 2006, **128**, 16398; (*b*) S. E. Bunn, C. T. Liu, Z.-L. Lu, A. A. Neverov and R. S. Brown, *J. Am. Chem. Soc.*, 2007, **129**, 16238; (*c*) C. T. Liu, A. A. Neverov and R. S. Brown, *J. Am. Chem. Soc.*, 2008, **130**, 16711; (*d*) A. A. Neverov, C. T. Liu, S. E. Bunn, D. Edwards, C. J. White, S. A. Melnychuk and R. S. Brown, *J. Am. Chem. Soc.*, 2008, **130**, 6639.
6 R. S. Brown and A. A. Neverov, *J. Chem. Soc., Perkin Trans. 2*, 2002, 1039.
7 J. S. Tsang, A. A. Neverov and R. S. Brown, *J. Am. Chem. Soc.*, 2003, **125**, 1559.
8 For a representative list of references on various dinuclear metal-containing complexes, see: (*a*) J. Weston, *Chem. Rev.*, 2005, **105**, 2151; (*b*) N. H. Williams, B. Takasaki, M. Wall and J. Chin, *Acc. Chem. Res.*, 1999, **32**, 485; (*c*) G. Feng, D. Natale, R. Prabaharan, J. C. Marque-Rivas and N. H. Williams, *Angew. Chem., Int. Ed.*, 2006, **45**, 7056; (*d*) M.-Y. Yang, O. Iranzo, J. P. Richard and J. R. Morrow, *J. Am. Chem. Soc.*, 2005, **127**, 1064; (*e*) O. Iranzo, T. Elmer, J. P. Richard and J. R. Morrow, *Inorg. Chem.*, 2003, **42**, 7737; (*f*) O. Iranzo, J. P. Richard and J. R. Morrow, *Inorg. Chem.*, 2004, **43**, 1743; (*g*) O. Iranzo, A. Y. Kovalevsky, J. R. Morrow and J. P. Richard, *J. Am. Chem. Soc.*, 2003, **125**, 1988; (*h*) F. Mancin, E. Rampazzo, P. Tecilla and U. Tonellato, *Eur. J. Org. Chem.*, 2004, 281; (*i*) M. Subat, K. Woinaroschy, C. Gerstl, B. Sarkar, W. Kaim and B. König, *Inorg. Chem.*, 2008, **47**, 4661; (*j*) H. Linjalahti, G. Feng, J. C. Marque-Rivas, S. Mikkola and N. H. Williams, *J. Am. Chem. Soc.*, 2008, **130**, 4232.
9 (*a*) R. S. Brown and A. A. Neverov, Adv. Phys. Org. Chem., Ed: J. P. Richard, Elsevier: San Diego, Calif, 2007, **42**, 271; (*b*) R. S. Brown, Z.-l. Lu, C. T. Liu, W. Y. Tsang, D. R. Edwards and A. A. Neverov, *J. Phys. Org. Chem.*, 2009, **23**, 1; R. S. Brown, *Progress in Inorganic Chemistry*, Ed: K. D. Karlin, John Wiley & Sons, 2012, **57**, 55.
10 J. Kim and H. Lim, *Bull. Korean Chem. Soc.*, 1999, **20**, 491.
11 (*a*) T. Gadja, T. Düpre, I. Török, J. Harmer, A. Schweiger, J. Sander, D. Kuppert and K. Hegetschweiler, *Inorg. Chem.*, 2001, **40**, 4918; (*b*) A. Jancsó, S. Mikkola, H. Lönnberg, K. Hegetschweiler and T. Gadja, *Chem.–Eur. J.*, 2003, **9**, 5404.
12 For a representative list of references on various mononuclear metal containing complexes, see: (*a*) M. Livieri, F. Mancin, U. Tonellato and J. Chin, *Chem. Commun.*, 2004, 2862; (*b*) G. Feng, J. C. Marque-Rivas and N. H. Williams, *Chem. Commun.*, 2006, 1845; (*c*) M. Livieri, F. Mancin, G. Saielli, J. Chin and U. Tonellato, *Chem.–Eur. J.*, 2007, **13**, 2246; (*d*) R. Bonomi, G. Saielli, U. Tonellato, P. Scrimin and F. Mancin, *J. Am. Chem. Soc.*, 2009, **131**, 11278; (*e*) L. Bonfa, M. Gatos, F. Mancin, P. Tecillaand and U. Tonellato, *Inorg. Chem.*, 2003, **42**, 3943; (*f*) T. Koike and E. Kimura, *J. Am. Chem. Soc.*, 1991, **113**, 8935.
13 K. A. Deal and J. N. Burstyn, *Inorg. Chem.*, 1996, **35**, 2792.
14 M. F. Mohamed, A. A. Neverov and R. S. Brown, *Inorg. Chem.*, 2009, **48**, 11425.
15 M. F. Mohamed and R. S. Brown, *J. Org. Chem.*, 2010, **75**, 8471.
16 W. Y. Tsang, D. R. Edwards, S. A. Melnychuk, C. T. Liu, C. Liu, A. A. Neverov, N. H. Williams and R. S. Brown, *J. Am. Chem. Soc.*, 2009, **131**, 4158.
17 P. C. Kunz, N. E. Brückmann and B. Spingler, *Eur. J. Inorg. Chem.*, 2007, 394.
18 J. Zhang, G. Leitus, Y. Ben-Davidand and D. Milstein, *J. Am. Chem. Soc.*, 2005, **127**, 10840.
19 B. de Bruin, J. A. Brands, J. J. J. M. Donners, M. P. J. Donners, R. de Gelder, J. M. M. Smits, A. W. Gal and A. L. Spek, *Chem.–Eur. J.*, 1999, **5**, 2921.
20 (*a*) G. Gibson, A. A. Neverov and R. S. Brown, *Can. J. Chem.*, 2003, **81**, 495; (*b*) For the designation of pH in non-aqueous solvents we use the nomenclature recommended by the IUPAC, *Compendium of Analytical Nomenclature. Definitive Rules 1997* 3rd edn, Blackwell, Oxford, UK, 1998. The pH meter reading for an aqueous solution determined with an electrode calibrated with aqueous buffers is designated as $^{w}_{w}$pH; if the electrode is calibrated in water and the 'pH' of the neat buffered methanol solution then measured, the term $^{s}_{w}$pH is used; and if the electrode is calibrated in the same solvent and the 'pH' reading is made, then the term $^{s}_{s}$pH is used. In methanol $^{s}_{w}$pH-(–2.24) = $^{s}_{s}$pH and since the autoprotolysis constant of methanol is $10^{-16.77}$, neutral $^{s}_{s}$pH is 8.4.
21 P. Gans, A. Sabatini and A. Vacca, *Talanta*, 1996, **43**, 1739.
22 J. S. Tsang, A. A. Neverov and R. S. Brown, *J. Am. Chem. Soc.*, 2003, **125**, 1559.
23 (*a*) A. J. Kirby and F. Hollfelder, *From Enzyme Models to Model Enzymes*, RSC Publishing, Cambridge, 2009, 1st edn, pp. 17–18; (*b*) M. I. Page, *Chem. Soc. Rev.*, 1973, **2**, 295; (*c*) M. I. Page and W. P. Jencks, *Proc. Natl. Acad. Sci. U. S. A.*, 1971, **68**, 1678.
24 A. J. Kirby and G. J. Lloyd, *J. Chem. Soc., Perkin Trans. 2*, 1976, 1753.
25 C. Tony Liu, Alexei A. Neverov and R. Stan Brown, *Inorg. Chem.*, 2007, **46**, 1778.